

Two-dimensional tunnel correlations with dissipation

A. K. Aringazin*

Department of Theoretical Physics, Institute for Basic Research, Eurasian National University, Astana 473021, Kazakhstan

Yuri Dahnovsky†

Department of Physics and Astronomy, P.O. Box 3905, University of Wyoming, Laramie, Wyoming 82071, USA

V. D. Krevchik‡ and M. B. Semenov§

Department of Physics, Penza State University, 40 Krasnaya St., Penza 440017, Russia

A. A. Ovchinnikov

Joint Institute of Chemical Physics, Kosygin Street 4, 117334 Moscow, Russia

K. Yamamoto

Research Institute of International Medical Center of Japan, Tokyo, Japan

(Received 28 December 2002; revised manuscript received 29 May 2003; published 28 October 2003)

Tunneling of two particles in synchronous and asynchronous regimes is studied in the framework of dissipative quantum tunneling. The critical temperature T_c corresponding to a bifurcation of the underbarrier trajectory is determined. The effect of a heat bath local mode on the probability of two-dimensional tunneling transfer is also investigated. At certain values of the parameters, the degeneracy of antiparallel tunneling trajectories is important. Thus, 4, 6, 12, etc., pairs of the trajectories should be taken into account (*a cascade of bifurcations*). For parallel particle tunneling the bifurcation resembles a phase transition of the first kind, while for antiparallel transfer it behaves as a second-order phase transition. The proposed theory allows for an explanation of experimental data on quantum fluctuations in two-proton tunneling in porphyrins near the critical temperature.

DOI: 10.1103/PhysRevB.68.155426

PACS number(s): 73.40.Gk, 82.20.Xr, 03.65.Xp, 31.15.Gy

I. INTRODUCTION

The quantum tunneling dynamics of a particle interacting with a heat bath is one of the important problems of modern condensed matter physics.^{1–30} The interest in this problem is related to studies of low-temperature superconductive tunnel junctions,^{5,6,9} dissipative quantum tunneling in crystals,¹³ and low-temperature chemical reactions.^{1,24–30} In low-dimensional systems an effective mass approximation often fails. Thus, quantum tunneling with dissipation becomes an important tool in the description of electron transfer.^{3,13} In many physical processes tunneling of *two* particles occurs. For example, Semenov and Dakhnovskii^{28,29} found the bistability of the tunneling trajectories in a two-proton transfer. Later, Benderskii and co-workers extended their investigations to different two-dimensional potentials.³⁰ Some features of the two-dimensional tunneling dynamics were studied in interacting Josephson junctions.⁶

Another example of two-particle tunneling is a two-proton transfer in porphyrin systems.^{27–29} Porphyrins are important molecules in biology³¹ and a new area of electronics: molecular wires and devices.³² There are experimental data^{24–26,33} that clearly indicate that a tunneling instability occurs at some critical temperature. Such a behavior in the rate constant demonstrates the existence of bifurcations in two-dimensional underbarrier trajectories. Apparently, this effect requires a thorough investigation when the protons interact with a thermal bath.

In this paper, we continue to study bifurcation effects in two-dimensional tunneling. In particular, we consider two-

proton correlations of different types within the framework of the dissipative quantum tunneling (instanton) approach. Moreover, we discuss the fine structure of bifurcations for systems with various potential energy surfaces.^{27–30,33,34} In Sec. II, we introduce two-dimensional model potential energy surfaces for a pair of interacting particles. In Sec. III, we study the effect of temperature on the tunneling rate. In Secs. IV and V, we calculate the rate for the parallel and antiparallel tunneling and provide an analysis of the origin of bifurcation. The effect of a promoting mode (an environment) is studied in Sec. VI.

II. TWO-DIMENSIONAL POTENTIAL ENERGY SURFACES

Consider two charges that tunnel in two independent double-well potentials $U(q_1)$ and $U(q_2)$ presented as follows:^{7,27–29}

$$\begin{aligned} \tilde{U}(q_i) = & \frac{1}{2} \omega^2 (q_i + a)^2 \theta(-q_i) \\ & + \left[-\Delta I + \frac{1}{2} \omega^2 (q_i - b)^2 \right] \theta(q_i), \quad i = 1, 2, \end{aligned} \quad (1)$$

where the sum $a + b$ determines the length of a “link” in the corresponding macrocluster fragment, $\Delta I = \omega^2 (b^2 - a^2)/2$ is a bias (an asymmetry parameter of the potential), $\theta(q_i)$ is a step function, and ω is the frequency (see discussion in Ref. 27). The mass is absorbed into the definition of q .

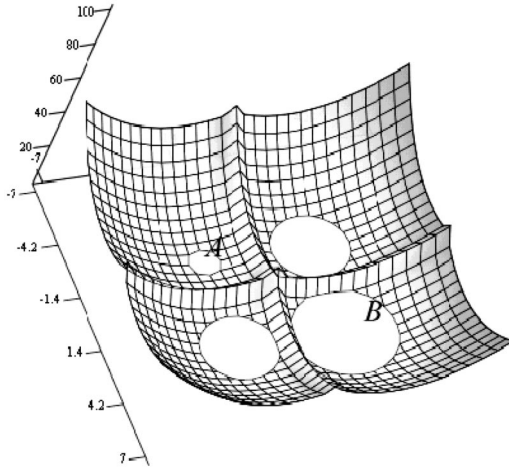


FIG. 1. Asymmetric potential energy surface (3) for parallel tunneling: $a=2$, $b=2.5$, $\alpha^*=0.0001$. A and B indicate the initial and final states of the particles, respectively. The minimum of the potential at B is lower than that at A . The other two (intermediate) minima are lower than those at A and higher than at B .

The interaction between two charges, e.g., protons, is considered in a dipole-dipole approximation²⁸

$$V_{\text{int}}(q_1, q_2) = -\frac{\alpha}{2}(q_1 - q_2)^2, \quad (2)$$

where α is a positive constant. We use the same interaction potential as in Ref. 6.

Thus, the total two-dimensional potential energy surface for parallel tunneling normalized by ω^2 is given by

$$\begin{aligned} U_p(q_1, q_2) &= \frac{2\tilde{U}_p(q_1, q_2)}{\omega^2} \\ &= (q_1 + a)^2 \theta(-q_1) + [-(b^2 - a^2) \\ &\quad + (q_1 - b)^2] \theta(q_1) + (q_2 + a)^2 \theta(-q_2) \\ &\quad + [-(b^2 - a^2) + (q_2 - b)^2] \theta(q_2) \\ &\quad - \frac{\alpha^*}{2}(q_1 - q_2)^2. \end{aligned} \quad (3)$$

Here, $\alpha^* = 2\alpha/\omega^2$ is the dimensionless parameter, $\alpha^* < 1$, $\alpha \approx e^2/(\epsilon R_0^3)$, e is the electron charge, R_0 is the separation distance between the reaction coordinates q_1 and q_2 of the tunneling particles, and ϵ is the dielectric constant. The form of the potential energy surface (3) is shown in Fig. 1.

For antiparallel transfer, the two-dimensional potential energy with the interaction term can be defined as

$$\begin{aligned} U_a(q_1, q_2) &= \frac{2\tilde{U}_a(q_1, q_2)}{\omega^2} = (q_1 + a)^2 \theta(-q_1) \\ &\quad + [-(b^2 - a^2) + (q_1 - b)^2] \theta(q_1) \\ &\quad + (q_2 - a)^2 \theta(q_2) + [-(b^2 - a^2) \\ &\quad + (q_2 + b)^2] \theta(-q_2) - \frac{\tilde{\alpha}^*}{2}(q_1 - q_2)^2, \end{aligned} \quad (4)$$

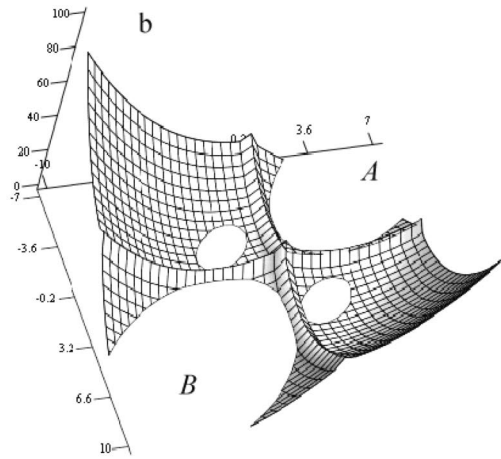
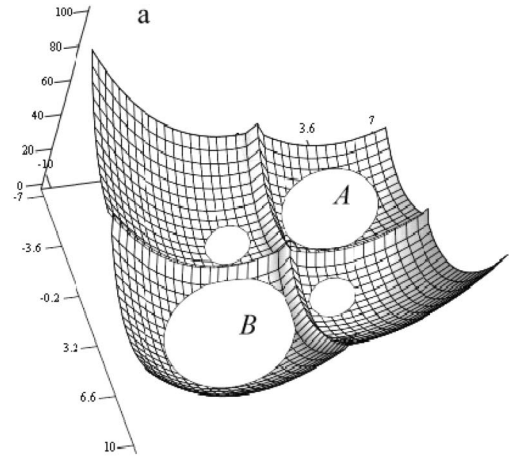


FIG. 2. Asymmetric potential energy surface (4) for antiparallel tunneling: (a) $a=2$, $b=2.3$, $\tilde{\alpha}^*=0.1$ (top panel); (b) $a=2$, $b=2.3$, $\tilde{\alpha}^*=0.5$ (bottom panel). A and B indicate initial and final states of the particles. The minimum of the potential at B is lower than that at A . The other two (intermediate) minima are higher than those at A and B .

where $\tilde{\alpha}^* = 2\tilde{\alpha}/\omega^2$ is a dimensionless parameter, $\tilde{\alpha}^* < 1$. The potential (4) is depicted in Fig. 2. The main difference between the potential energy surfaces (3) and (4) is in the initial location of the second particle, $\pm a$.

The potential energy (3) can be referred to as ‘‘parallel’’ while the potential energy (4) as ‘‘antiparallel.’’ We also define a ‘‘symmetric’’ potential energy as a particular case of the potential (4) under the condition $a=b$, i.e.,

$$\begin{aligned} U_s(q_1, q_2) &= \frac{2\tilde{U}_s(q_1, q_2)}{\omega^2} = (q_1 + a)^2 \theta(-q_1) \\ &\quad + (q_1 - a)^2 \theta(q_1) + (q_2 - a)^2 \theta(q_2) \\ &\quad + (q_2 + a)^2 \theta(-q_2) - \frac{\tilde{\alpha}^{**}}{2}(q_1 - q_2)^2, \end{aligned} \quad (5)$$

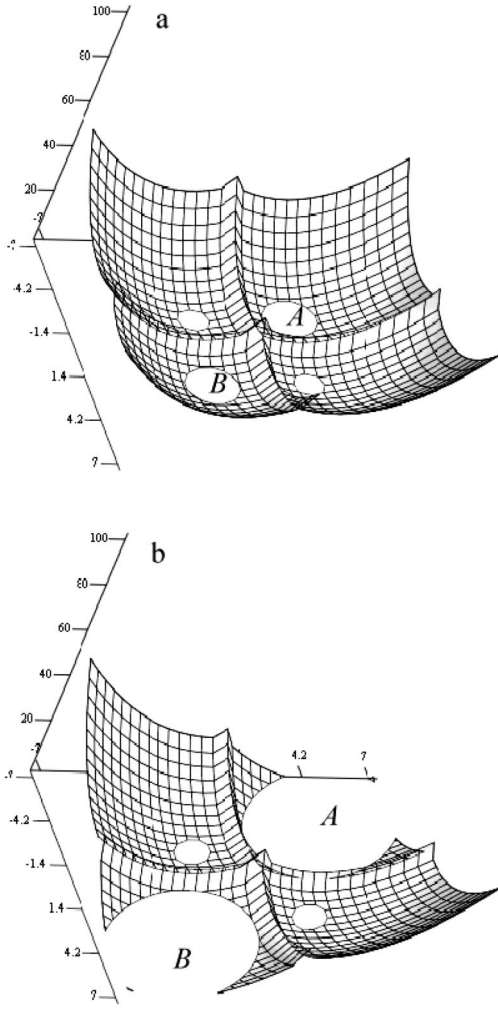


FIG. 3. Symmetric potential energy surface (5): (a) $a=2$, $b=2$, $\tilde{\alpha}^{**}=0.1$ (top panel); (b) $a=2$, $b=2$, $\tilde{\alpha}^{**}=0.5$ (bottom panel). A and B denote the initial and final states of the particles. The minimum of the potential energy at B is equal to that at A . The other two (intermediate) minima are higher than those at A and B .

where the constant $\tilde{\alpha}^{**} < 1$. The potential energy (5) is presented in Fig. 3.

As shown in Refs. 28, 29, and 33, such model potential energy surfaces describe well the dynamics in porphyrins.

In many practical cases, the effect of a bath on the particle tunneling should be also included. In the next section we consider two particles embedded in a harmonic medium and linearly interacting with the bath modes.

III. TWO-PARTICLE TRANSITION PROBABILITY

We assume that two particles independently interact with a harmonic bath. Such an interaction is considered in a bilinear approximation. The dynamics of the environment is described by the oscillator Hamiltonian (we use $\hbar=1$, $k_B=1$ units with the oscillator masses equal to 1)

$$H_{\text{ph}} = \frac{1}{2} \sum_i (P_i^2 + \omega_i^2 Q_i^2). \quad (6)$$

Each of the tunneling particles (electrons or effective charges) interacts with the oscillator bath in the following way:

$$V_{\text{p-ph}}^{(1)}(q_1, Q_i) = q_1 \sum_i C_i Q_i, \quad V_{\text{p-ph}}^{(2)}(q_2, Q_i) = q_2 \sum_i C_i Q_i. \quad (7)$$

As in Ref. 28, we are interested in the transition probability per unit time or, more precisely, only in its exponential part which can be written in the Langer's form

$$\Gamma = 2T \frac{\text{Im} Z}{\text{Re} Z}. \quad (8)$$

In such a consideration, metastable levels can be presented as

$$\Gamma = -2 \text{Im} E, \quad E = E_0 - i\Gamma/2. \quad (9)$$

It should be emphasized that Eq. (8) is valid only for temperatures below the crossover temperature while for higher temperatures a different prefactor is required.²³

Equation (8) is obtained by generalizing the expression (9) to nonzero temperatures:²⁻¹⁷

$$\Gamma = \frac{2 \sum_i e^{-E_{0i}/T} \text{Im} E_i}{e^{-E_{0i}/T}} = \frac{2T \text{Im} \sum_i e^{-E_i/T}}{\text{Re} \sum_i e^{-E_i/T}} = \frac{2T \text{Im} Z}{\text{Re} Z}. \quad (10)$$

Here i labels the energy levels in the metastable state, Z is the partition function of the system, and T is the temperature.

To calculate Γ , it is convenient to present Z in the form of a path integral²⁻¹⁷

$$Z = \prod_i \int Dq_1 Dq_2 DQ_i \exp[-S\{q_1, q_2, Q_i\}]. \quad (11)$$

Here S denotes an underbarrier action for the total system. The imaginary part $\text{Im} Z$ is due to the decay of the energy states in the initial well. The validity of this approximation requires dissipation to be strong enough so that only an incoherent decay occurs.²³ The imaginary part in the partition function with a double-well potential energy can be also explained due to the strong dissipation to the bath. Indeed, the particles do not come back to their initial state. Coherent oscillations can happen only if the interaction with bosons is weak enough⁸ or the bath is in nonequilibrium state.^{35,37}

The integral (11) can be performed over phonon coordinates,²⁸ resulting in

$$S\{q_1, q_2\} = \int_{-\beta/2}^{\beta/2} d\tau \left[\frac{1}{2} \dot{q}_1^2 + \frac{1}{2} \dot{q}_2^2 + V(q_1, q_2) \right. \\ \left. + \int_{-\beta/2}^{\beta/2} d\tau' D(\tau - \tau') [q_1(\tau) + q_2(\tau)] \right. \\ \left. \times [q_1(\tau') + q_2(\tau')] \right], \quad (12)$$

where

$$D(\tau) = \frac{1}{\beta} \sum_{n=-\infty}^{\infty} D(\nu_n) e^{i\nu_n \tau}, \quad (13)$$

$\beta = \hbar/(k_B T)$ is an inverse temperature (below we assume that $\hbar = 1$ and $k_B = 1$), $\nu_n = 2\pi n/\beta$ is the Matsubara's frequency, and

$$D(\nu_n) = - \sum_i \frac{C_i^2}{\omega_i^2 + \nu_n^2}. \quad (14)$$

A trajectory that minimizes the Euclidean action S can be found from the equations of motion. In particular, we embark on the antiparallel tunneling

$$-\ddot{q}_1 + \Omega_0^2 q_1 + \tilde{\alpha}_1 q_2 + \int_{-\beta/2}^{\beta/2} d\tau' K(\tau - \tau') [q_1(\tau') + q_2(\tau')] + \omega^2 a \theta(-q_1) - \omega^2 b \theta(q_1) = 0, \quad (15)$$

$$-\ddot{q}_2 + \Omega_0^2 q_2 + \tilde{\alpha}_1 q_2 + \int_{-\beta/2}^{\beta/2} d\tau' K(\tau - \tau') [q_1(\tau') + q_2(\tau')] - \omega^2 a \theta(q_2) + \omega^2 b \theta(-q_2) = 0. \quad (16)$$

In Eqs. (15) and (16) the kernel K is defined by

$$K(\tau) = \frac{1}{\beta} \sum_{n=-\infty}^{\infty} \xi_n e^{i\nu_n \tau}. \quad (17)$$

Here ξ_n is the Green's function defined by Eq. (14) without the zero-frequency term,

$$D(\nu_n) = - \sum_i \frac{C_i^2}{\omega_i^2} + \xi_n. \quad (18)$$

Thus, we seek solutions of Eqs. (15) and (16) by expanding the trajectories $q_1(t)$ and $q_2(t)$ into Fourier series,

$$q_1 = \frac{1}{\beta} \sum_{n=-\infty}^{\infty} q_n^{(1)} e^{i\nu_n \tau}, \quad q_2 = \frac{1}{\beta} \sum_{n=-\infty}^{\infty} q_n^{(2)} e^{i\nu_n \tau}. \quad (19)$$

Introducing the renormalized frequency and interaction constant

$$\Omega_0^2 = \omega^2 - \sum_i \frac{C_i^2}{\omega_i^2} - \tilde{\alpha}, \quad \tilde{\alpha}_1 = \tilde{\alpha} - \sum_i \frac{C_i^2}{\omega_i^2}, \quad (20)$$

respectively, and substituting Eqs. (19) into Eqs. (15) and (16), we obtain that, for $n=0$,

$$q_0^{(1)} + q_0^{(2)} = \frac{2\omega^2(a+b)\varepsilon}{\Omega_0^2 + \tilde{\alpha}_1},$$

$$q_0^{(1)} - q_0^{(2)} = - \frac{2\omega^2 a \beta}{\Omega_0^2 - \tilde{\alpha}_1} + \frac{4\omega^2(a+b)\tau_0}{\Omega_0^2 - \tilde{\alpha}_1}, \quad (21)$$

and, for $n \neq 0$,

$$q_n^{(1)} + q_n^{(2)} = \frac{2\omega^2(a+b)(\sin \nu_n \tau_1 - \sin \nu_n \tau_2)}{\nu_n(\nu_n^2 + \Omega_0^2 + \tilde{\alpha}_1 + 2\xi_n)},$$

$$q_n^{(1)} - q_n^{(2)} = \frac{2\omega^2(a+b)(\sin \nu_n \tau_1 + \sin \nu_n \tau_2)}{\nu_n(\nu_n^2 + \Omega_0^2 - \tilde{\alpha}_1)}. \quad (22)$$

Here we have introduced the following notation:

$$\varepsilon = \tau_1 - \tau_2, \quad \tau_0 = (\tau_1 + \tau_2)/2. \quad (23)$$

The time instants τ_1 and τ_2 , at which the particles pass the top points of the barrier, are determined from the following equations:

$$q_1(\tau_1) = 0, \quad q_2(\tau_2) = 0. \quad (24)$$

Equations (24) allow us to change the argument of the θ function. Namely, instead of the q_1 and q_2 dependences, we can use a time-dependent θ function. This reduces Eqs. (15) and (16) to a linear form.

Finally, substituting the trajectory determined from Eqs. (19), (21), and (22) into Eq. (12), we arrive at the following expression for the instanton action:

$$S = \frac{4\omega^4(a+b)\tau_0}{\Omega_0^2 - \tilde{\alpha}_1} - \frac{\omega^4(a+b)^2\varepsilon^2}{\beta(\Omega_0^2 + \tilde{\alpha}_1)} - \frac{4\omega^4(a+b)^2\tau_0^2}{\beta(\Omega_0^2 - \tilde{\alpha}_1)} - \frac{8\omega^4(a+b)^2}{\beta} \sum_{n=1}^{\infty} \left[\frac{\sin^2 \nu_n \tau_0 \cos^2(\nu_n \varepsilon/2)}{(\nu_n^2 + \Omega_0^2 - \tilde{\alpha}_1)\nu_n^2} + \frac{\cos^2 \nu_n \tau_0 \sin^2(\nu_n \varepsilon/2)}{(\nu_n^2 + \Omega_0^2 + \tilde{\alpha}_1 + 2\xi_n)\nu_n^2} \right]. \quad (25)$$

IV. PARALLEL PARTICLE TUNNELING

For the case of parallel particle tunneling, the Euclidean action S can be determined similarly to antiparallel tunneling [see Eqs. (15) and (16)]. The trajectory minimizing the Euclidean action (instanton) can be determined from the equations of motion. As in the previous section, we seek solutions of these equations in the form of the Fourier expansion (19). The time instants τ_1 and τ_2 are determined by Eqs. (24).

In the case of parallel tunneling particles [the potential energy (3)], the resulting Euclidean action is given as follows:

$$S = 2a(a+b)(\tau_1 + \tau_2)\omega^2 - \frac{1}{\beta}\omega^2(a+b)^2(\tau_1 + \tau_2)^2 - \frac{\omega^4(a+b)^2(\tau_1 - \tau_2)^2}{(\omega^2 - 2\alpha)\beta} - \frac{2\omega^4(a+b)^2}{\beta} \sum_{n=1}^{\infty} \left[\frac{(\sin \nu_n \tau_1 + \sin \nu_n \tau_2)^2}{\nu_n^2(\nu_n^2 + \omega^2 + \xi_n)} + \frac{(\sin \nu_n \tau_1 - \sin \nu_n \tau_2)^2}{\nu_n^2(\nu_n^2 + \omega^2 - 2\alpha)} \right], \quad (26)$$

where ξ_n is defined by Eq. (18).

Below, we use the following notation:

$$\varepsilon = \varepsilon^* \omega = (\tau_1 - \tau_2) \omega,$$

and assume that

$$\tau = 2\tau^* \omega = (\tau_1 + \tau_2) \omega,$$

$$b \geq a.$$

$$\beta^* = \beta \omega / 2,$$

$$\alpha^* = 2\alpha / \omega^2,$$

$$b^* = b/a,$$

In the absence of interaction with an oscillator bath, i.e., at $\xi_n = 0$, the action (26) as a function of the parameters ε and τ yields

$$S = \frac{(a+b)^2 \omega}{2} \left\{ \frac{4a\tau}{a+b} - \frac{\tau}{a+b} \left(1 + \frac{1}{1-\alpha^*} \right) + \frac{(\tau - |\varepsilon|) \alpha^*}{1-\alpha^*} + \coth \beta^* - \sinh^{-1} \beta^* [\cosh(\beta^* - \tau) \cosh \varepsilon + \cosh(\beta^* - \tau) - \cosh(\beta^* - |\varepsilon|)] - (1-\alpha^*)^{-3/2} (-\coth(\beta \sqrt{1-\alpha^*}) + \sinh^{-1}(\beta \sqrt{1-\alpha^*}) \{ \cosh[(\beta^* - \tau) \sqrt{1-\alpha^*}] [\cosh(\varepsilon \sqrt{1-\alpha^*}) - 1] + \cosh[(\beta^* - |\varepsilon|) \sqrt{1-\alpha^*}] \} \right) \right\}. \quad (27)$$

As soon as the trajectory is found, Eqs. (24) can be presented in the following form:

$$\begin{aligned} & \sinh \varepsilon [\cosh \tau \coth \beta^* - \sinh \tau - \coth \beta^*] + \frac{1}{1-\alpha^*} \sinh(\varepsilon \sqrt{1-\alpha^*}) [\cosh(\tau \sqrt{1-\alpha^*}) \coth(\beta^* \sqrt{1-\alpha^*}) - \sinh(\tau \sqrt{1-\alpha^*}) \\ & + \coth(\beta^* \sqrt{1-\alpha^*})] = 0, \quad 3 - \frac{4}{1+b^*} - \frac{1}{1-\alpha^*} + \cosh \varepsilon [\sinh \tau \coth \beta^* - \cosh \tau - 1] + \sinh \tau \coth \beta^* - \cosh \tau \\ & + \frac{1}{1-\alpha^*} \cosh(\varepsilon \sqrt{1-\alpha^*}) [\sinh(\tau \sqrt{1-\alpha^*}) \coth(\beta^* \sqrt{1-\alpha^*}) - \cosh(\tau \sqrt{1-\alpha^*}) + 1] \\ & - \frac{1}{1-\alpha^*} [\sinh(\tau \sqrt{1-\alpha^*}) \coth(\beta^* \sqrt{1-\alpha^*}) - \cosh(\tau \sqrt{1-\alpha^*})] = 0. \end{aligned} \quad (28)$$

Simple analytic solutions of Eqs. (28) are obtained in the particular case when

$$\varepsilon = (\tau_1 - \tau_2) \omega = 0, \quad \forall \beta, \quad \alpha < \omega^2 / 2,$$

$$\tau_1 = \tau_2 = \frac{\tau}{2\omega} = \frac{1}{2\omega} \operatorname{arcosh} \left[\frac{1-b^*}{1+b^*} \sinh \frac{\beta \omega}{2} \right] + \frac{\beta}{4}. \quad (29)$$

However, a complete analysis requires numerical studies.

At sufficiently low temperatures, $\omega \beta \gg 1$, for $1 < b/a < 3$, and

$$\frac{b-a}{2(b+a)} \leq \frac{2\alpha}{\omega^2} < \alpha_c^* \equiv \frac{2(b-a)}{3b-a},$$

we finally obtain, with exponential accuracy,

$$\begin{aligned} e^{-\tau \sqrt{1-\alpha^*}} & \simeq \left[3 - \frac{4}{1+b^*} - \frac{1}{1-\alpha^*} \right] (1-\alpha^*)^{1/(1-\sqrt{1-\alpha^*})} \left\{ 1 + (1-\alpha^*)^{1/(1-\sqrt{1-\alpha^*})} \right. \\ & \left. \times \left[-\frac{1}{1-\alpha^*} + \left(3 - \frac{4}{1+b^*} - \frac{1}{1-\alpha^*} \right) / (1-\sqrt{1-\alpha^*}) \right] \right\}^{-1}, \quad e^{-\varepsilon} \simeq \left[3 - \frac{4}{1+b^*} - \frac{1}{1-\alpha^*} \right] e^{\tau \sqrt{1-\alpha^*}} + \frac{1}{1-\alpha^*}. \end{aligned} \quad (30)$$

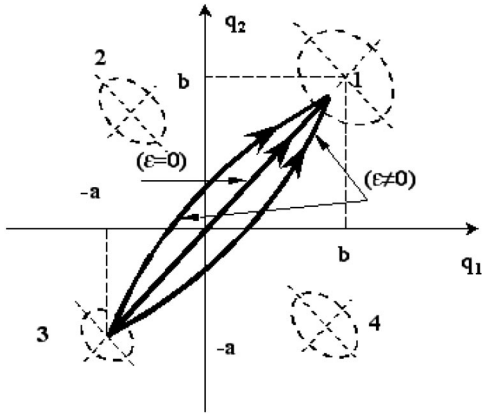


FIG. 4. Trajectories (a single path is characterized by $\varepsilon=0$ and a split path is characterized by $\varepsilon \neq 0$) for two parallel moving particles, at $\omega\beta \gg 1$. (1)–(4) label the projections of the minima of potential energy (3).

The solution (30) is valid at

$$\beta > \beta_c \equiv \frac{\tau \sqrt{1 - \alpha^*}}{\omega}. \quad (31)$$

We point out that an approximate solution can be found for large values of the parameter b^* (and small α^*). However, below we focus on the more important solution (30). The analysis indicates that there are no perturbative solutions of Eqs. (28) at low temperatures and small ε .

For $\varepsilon=0$ [see Eq. (29)], the action (27) results in

$$\begin{aligned} S_{\varepsilon=0} &= \omega(b^2 - a^2) \operatorname{arcosh} \left[\frac{b^* - 1}{b^* + 1} \sinh \frac{\omega\beta}{2} \right] \\ &\quad - \frac{1}{2} \omega^2 (b^2 - a^2) \beta + \omega(b+a)^2 \\ &\quad \times \left[\cosh \frac{\omega\beta}{2} \left(1 + \frac{(b^* - 1)^2}{(b^* + 1)^2} \sinh^2 \frac{\omega\beta}{2} \right)^{1/2} \right] \\ &\quad \times \sinh^{-1} \frac{\omega\beta}{2}. \end{aligned} \quad (32)$$

The action (32) coincides (up to a factor of 2) with that of calculated in Ref. 27. Thus, we have calculated the two-particle Euclidean action for the case of synchronous parallel motion of the two interacting particles.

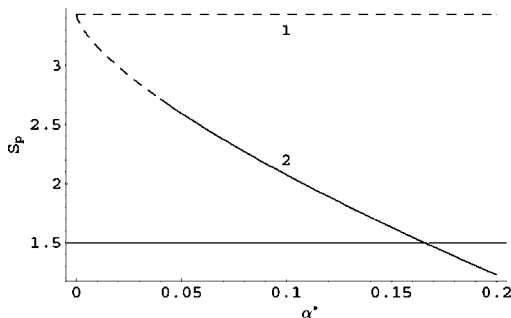


FIG. 5. Instanton action as a function of the interaction parameter $\alpha^* = 2\alpha/\omega^2$ of the two parallel moving particles, at $\omega\beta \gg 1$; $S_p = S/(\omega a^2)$. (1) is the single trajectory; (2) is the split trajectory.

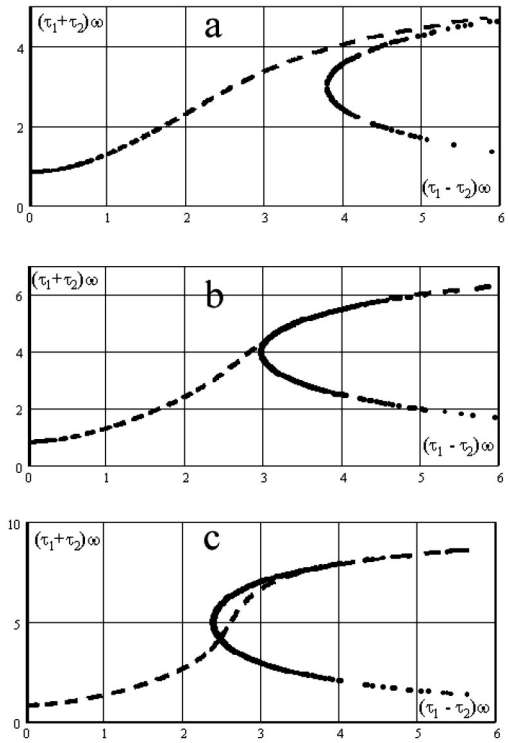


FIG. 6. Numerical solutions of transcendental equations (28). In addition to the studied solution $\tau_1 = \tau_2$, with larger β there are additional solutions, $\tau_1 \neq \tau_2$, shown in panels (b) and (c). Panel (b) reveals a *single* additional solution corresponding to the lower value of the Euclidean action. Panel (c) shows two different additional solutions with the one corresponding to the lower value of the action.

In the symmetric case ($b^* = 1$), the action (32) reduces to

$$S_{\varepsilon=0} = 4\omega^2 \tanh \frac{\omega\beta}{4}. \quad (33)$$

At $b^* > 1$, the character of the temperature dependence is almost the same.

At $\varepsilon \neq 0$, the corresponding action S can be obtained by substituting Eq. (30) into Eq. (27) (for brevity, this cumbersome expression is omitted). A simple analysis shows that $S_{\varepsilon \neq 0} < S_{\varepsilon=0}$. Moreover, it appears that the difference $\Delta S = S_{\varepsilon \neq 0} - S_{\varepsilon=0}$ has a maximum at $\omega\beta \gg 1$.

The tunneling paths (19) are presented by the solutions (29) and (30). At the critical point $\beta = \beta_c$, defined by Eq. (31), a relatively abrupt change in the dynamics results in a splitting of the single trajectory ($\varepsilon=0$) into two ($\varepsilon \neq 0$), as shown in Fig. 4.

At $\beta > \beta_c$, i.e., for temperatures below the critical temperature, $T < T_c$, only a split trajectory ($\varepsilon \neq 0$) occurs since $S_{\varepsilon \neq 0} < S_{\varepsilon=0}$ (see Fig. 5).

When $\beta < \beta_c$, i.e., at $T > T_c$, and $\alpha > \alpha_c$ [see Eq. (30)], the solution is determined by a single trajectory. We have also found that the single-trajectory solution holds in the whole temperature range for a symmetric potential energy ($b^* = 1$).

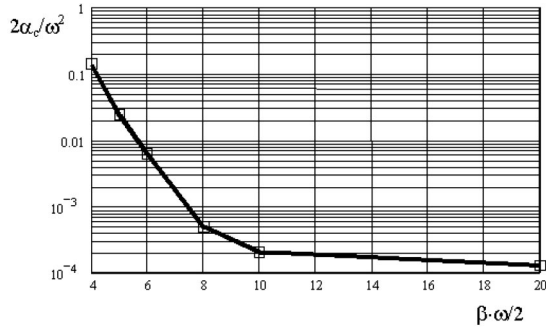


FIG. 7. Parameter α_c as a function of inverse temperature, at a fixed value of the frequency ω and asymmetry parameter b^* .

The above consideration is based on the analytic solutions (29) for $\tau_{1,2}$ near the critical point. A complete analysis of Eq. (28) requires more detail.

The numerical study of the set of transcendental equations (28) reveals remarkable features of two-dimensional tunneling. The value of the critical parameter α_c decreases with temperature as shown in Figs. 6, 7, and 8. The temperature dependence of α_c indicates to the existence of a finite low-temperature limit. It becomes clear that the weaker the interaction between the tunneling particle, the lower temperatures required for the synchronous tunneling. Since the asynchronous tunneling is valid only for $T < T_c$ [see Eq. (31)], the dependence of β_c on the interaction parameter reveals that the minimum occurs at $\alpha^* = 0.2$. The nonmonotonic behavior of β_c as a function of α^* can be explained by the α^* dependence of τ as well.

Additionally, the curve in Fig. 8 exhibits an anomalous behavior (an increasing part of the curve) that can be explained in the following way: a two-dimensional potential energy for parallel tunneling is evidently deformed by an increase of the interaction constant. Indeed, the minima of the potential surface become lower and the distance between them is larger. Small deformations in the potential energy surface change the contribution produced by the temperature increase towards a synchronous character of the tunneling. However, for sufficiently large deformations of the potential, the situation is a quite opposite. The significant deformations are in favor of synchronous transfer. Thus, an increase in the interaction constant provides a similar effect when temperature increases. Such a behavior takes place up to a certain value of the interaction constant, beyond which the potential energy surface becomes strongly perturbed. Thus, Figs. 7 and 8 are complimentary to each other. Consequently, Fig. 8 can be viewed as a bifurcation diagram. Indeed, the region below

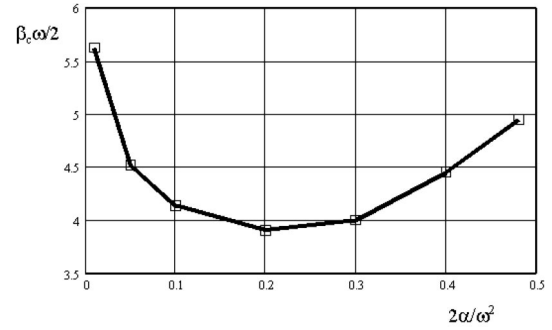


FIG. 8. Parameter β_c is presented as a function of the interaction parameter of the two tunneling particles.

the curve corresponds to the synchronous tunneling, while the region above the curve corresponds to the asynchronous one.

Figure 6 demonstrates how the critical parameter β_c changes from synchronous to asynchronous values with temperature. Figures 6(b) and 6(c) reveal the existence of additional points, referred to as bifurcation points, corresponding to the change of tunneling regimes. For the two bifurcation points shown in Fig. 6(c), only one is physical because it corresponds to the lower value of the action (the second point is metastable). However, for sufficiently small differences between the values of the action at these bifurcation points, *both* close points contribute, thus leading to corresponding “fluctuations” in the system during the change of the regimes. For lower temperatures, such fluctuations become negligible because two bifurcation points contribute differently. Thus, a stable character of the asynchronous tunnel transfer is achieved due to a much lower value of the action at one of the bifurcation points.

For the chemical reactions mentioned in Introduction, the effect of the change in the tunneling regimes reveals a *cleavage* in the experimental temperature dependence of the tunneling constant. The fine details of this instability have not been studied yet. Nevertheless, the very existence of an instability at the edge of the bifurcation can be explained as the result of specific fluctuations. A numerical analysis of the bifurcations in antiparallel tunneling is given in the next section.

V. TWO-DIMENSIONAL ANTIPARALLEL TUNNELING

For antiparallel tunneling of two particles [see the potential energy (4)], the instanton action as a function of the parameters ε and τ is determined by Eq. (25). For $\xi_n = 0$, we obtain

$$S = -\frac{\omega\tau(b^2 - a^2)}{1 - \tilde{\alpha}^*} - \frac{\omega(a+b)^2}{2} \left\{ |\varepsilon| \left(1 - \frac{1}{1 - \tilde{\alpha}^*} \right) + \frac{\sinh(|\varepsilon| \sqrt{1 - \tilde{\alpha}^*})}{(1 - \tilde{\alpha}^*)^{3/2}} - \sinh|\varepsilon| + \frac{\cosh(\varepsilon \sqrt{1 - \tilde{\alpha}^*}) + 1}{(1 - \tilde{\alpha}^*)^{3/2}} \right. \\ \left. \times [\sinh(\beta^* \sqrt{1 - \tilde{\alpha}^*})]^{-1} [\cosh((\beta^* - \tau) \sqrt{1 - \tilde{\alpha}^*}) - \cosh(\beta^* \sqrt{1 - \tilde{\alpha}^*})] + \frac{\cosh \varepsilon - 1}{\sinh \beta^*} [\cosh(\beta^* - \tau) + \cosh \beta^*] \right\}. \quad (34)$$

The parameters ε and τ are found from the following set of equations [see Eq. (24)]:

$$\begin{aligned}
& -\sinh \varepsilon [\coth \beta^* + \cosh \tau \coth \beta^* - \sinh \tau] + \frac{1}{1-\tilde{\alpha}^*} \sinh(\varepsilon \sqrt{1-\tilde{\alpha}^*}) [\coth(\beta^* \sqrt{1-\tilde{\alpha}^*}) - \cosh(\tau \sqrt{1-\tilde{\alpha}^*}) \coth(\beta^* \sqrt{1-\tilde{\alpha}^*}) \\
& + \sinh(\tau \sqrt{1-\tilde{\alpha}^*})] = 0, \quad -1 - \frac{4}{(1+b^*)(1-\tilde{\alpha}^*)} + \frac{1}{1-\tilde{\alpha}^*} + (\cosh \varepsilon - 1)(\sinh \tau \coth \beta^* - \cosh \tau) + \cosh \varepsilon \\
& + \frac{1}{1-\tilde{\alpha}^*} \{ [\cosh(\varepsilon \sqrt{1-\tilde{\alpha}^*}) + 1] [\sinh(\tau \sqrt{1-\tilde{\alpha}^*}) \coth(\beta^* \sqrt{1-\tilde{\alpha}^*}) - \cosh(\tau \sqrt{1-\tilde{\alpha}^*})] - \cosh(\varepsilon \sqrt{1-\tilde{\alpha}^*}) \} = 0. \quad (35)
\end{aligned}$$

Simple analytic solutions of Eqs. (35) can be obtained in the following form:

$$\varepsilon = (\tau_1 - \tau_2)\omega = 0, \quad \forall \beta, \quad \tilde{\alpha} < \omega^2/2,$$

$$\begin{aligned}
\tau_1 = \tau_2 &= \frac{\tau}{2\omega} \\
&= \frac{1}{2\omega \sqrt{1-\tilde{\alpha}^*}} \operatorname{arcosh} \left[\frac{1-b^*}{1+b^*} \sinh \left(\frac{\beta\omega}{2} \sqrt{1-\tilde{\alpha}^*} \right) \right] + \frac{\beta}{4}. \quad (36)
\end{aligned}$$

Similarly to the case of parallel tunneling, we obtain that at low temperatures, $\omega\beta \gg 1$, with exponential accuracy,

$$\begin{aligned}
e^{-\tau\sqrt{1-\tilde{\alpha}^*}} &\simeq \frac{A(1-\tilde{\alpha}^*)^{1/\gamma}}{1-(1-\tilde{\alpha}^*)^{1/\gamma}[A/\gamma-(1-\tilde{\alpha}^*)^{-1}]}, \\
e^\varepsilon &\simeq A e^{\tau\sqrt{1-\tilde{\alpha}^*}} - \frac{1}{1-\tilde{\alpha}^*}. \quad (37)
\end{aligned}$$

Here

$$A = -1 - \frac{4}{(1+b^*)(1-\tilde{\alpha}^*)} + \frac{3}{1-\tilde{\alpha}^*}, \quad \gamma = 1 - \sqrt{1-\tilde{\alpha}^*},$$

while $\tilde{\alpha}^*$, b^* , ε , and τ are determined as for the parallel transfer.

The solution (37) is valid at $\tilde{\alpha}_{c1}^* < \tilde{\alpha}^* < \tilde{\alpha}_{c2}^*$, where the lower and upper bounds $\tilde{\alpha}_{c1}^*$ and $\tilde{\alpha}_{c2}^*$ are derived from a cumbersome transcendental equation (for brevity it is not presented here). Particularly, in the symmetric case $b^*=1$, we obtain the condition in a simple analytic form $1/4 < 2\tilde{\alpha}/\omega^2 < 1$.

Furthermore, an approximate solution can be found for large values of the parameter $b^*=b/a$ (and small $\tilde{\alpha}^*$). However, we restrict our analysis to the more important physical solution (37).

The β -dependent solution (37) is valid for $\beta > \tilde{\beta}_c$, where

$$\tilde{\beta}_c \equiv -\frac{1}{\omega \sqrt{1-\tilde{\alpha}^*}} \ln \frac{A(1-\tilde{\alpha}^*)^{1/\gamma}}{1-(1-\tilde{\alpha}^*)^{1/\gamma} \left(\frac{A}{\gamma} - \frac{1}{1-\tilde{\alpha}^*} \right)}. \quad (38)$$

At $\omega\beta \gg 1$, the solutions of Eqs. (35) can be found perturbatively (for small ε) with given values of the parameters $(b-a)/(b+a)$ and $\tilde{\alpha}^*$. At $\varepsilon=0$ [the solution (36)], the action (34) yields

$$\begin{aligned}
S &= \frac{\omega(b^2-a^2)}{(1-\tilde{\alpha}^*)^{3/2}} \operatorname{arcosh} \left[\frac{b-a}{b+a} \sinh \frac{\omega\beta\sqrt{1-\tilde{\alpha}^*}}{2} \right] \\
&- \frac{\omega^2\beta(b^2-a^2)}{2(1-\tilde{\alpha}^2)} + \frac{\omega(b+a)^2}{(1-\tilde{\alpha}^*)^{3/2}} \left[\coth \frac{\omega\beta\sqrt{1-\tilde{\alpha}^*}}{2} \right. \\
&\left. - \left(\sinh^{-2} \frac{\omega\beta\sqrt{1-\tilde{\alpha}^*}}{2} + \frac{(b-a)^2}{(b+a)^2} \right)^{1/2} \right]. \quad (39)
\end{aligned}$$

For the symmetric potential ($a=b$) and $\varepsilon=0$, we obtain that (see Fig. 7)

$$S = \frac{4\omega a^2}{(1-\tilde{\alpha}^*)^{3/2}} \tanh \frac{\omega\beta\sqrt{1-\tilde{\alpha}^*}}{4}. \quad (40)$$

We do not present here a cumbersome expression for $S_{\varepsilon \neq 0}$ which one can obtain by substituting the solutions τ and ε into Eq. (34). A simple analysis reveals that $S_{\varepsilon \neq 0} > S_{\varepsilon=0}$ for $\beta > \tilde{\beta}_c$ and for relevant $\tilde{\alpha}^*$. Similarly to parallel transfer, the tunnel paths can be found from Eqs. (36) and (37). These trajectories on the (q_1, q_2) plane are shown in Fig. 9.

As for parallel tunneling and at $\beta > \tilde{\beta}_c$, the pair tunneling changes from a single- to a double-trajectory regime. In contrast to the parallel tunneling, such a splitting occurs at any values of the parameters of the potential. At $\beta > \tilde{\beta}_c$, we have $S_{\varepsilon \neq 0} > S_{\varepsilon=0}$ and, therefore, $S_{\varepsilon=0}$ determines the tunneling rate. At $\beta < \tilde{\beta}_c$, the two degenerated trajectories are transformed into a single trajectory, $q_1 = -q_2$, corresponding to synchronous antiparallel transfer.

For single-particle tunneling, there is only a single tunneling path (instanton) minimizing the action. Hence, there are two different types of trajectories for the pair of interacting particles. Namely, the main contribution to the instanton ac-

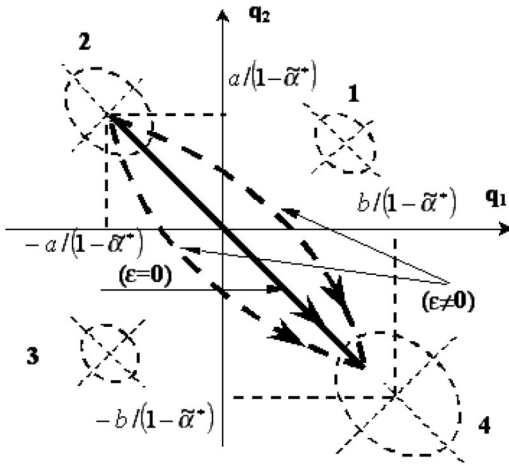


FIG. 9. Trajectories (the basic path characterized by $\varepsilon=0$ and the split one characterized by $\varepsilon \neq 0$) at $\omega\beta \gg 1$ of two antiparallel tunneling particles. (1)–(4) denote the projections of the minima of the potential energy surface $U_a(q_1, q_2)$ defined by Eq. (4).

tion is determined by either the single- or double-degenerated path depending on the value of β . We also point out that in the case of parallel tunneling, the particles do not simultaneously pass the top points of the barrier, $\tau_1 \neq \tau_2$, for $\beta > \beta_c$. This means that the tunneling transfer is asynchronous.

At small values of the interaction parameter α^* [see Eq. (30)] and at temperatures such that $\beta < \beta_c$ [see Eq. (31)], there is no splitting of a single path ($q_1 = q_2$). Therefore, the particles pass the top of the barriers at the same instants ($\tau_1 = \tau_2$). Consequently, the transfer of the particles is synchronous. The temperature dependence for the antiparallel transfer action is plotted in Fig. 10 at various $\tilde{\alpha}^*$.

The type of the interaction given by Eqs. (2)–(5) is such that it does not affect the motion along the “center-of-mass” coordinate, $q_1 = q_2$. For this reason, the Euclidean action is independent of the interaction parameter as for parallel transfer. Since the state of the interacting system characterized by a maximal value of the relative coordinate, $q_1 = -q_2$, is preferable (as it provides the lower action), it becomes clear that the instanton action decreases with the interaction parameter in the parallel transfer along the degenerated tunnel trajectories and increases with the interaction parameter for the antiparallel tunneling.

For antiparallel tunneling, synchronous transfer ($\tau_1 = \tau_2$) takes place, while asynchronous transfer is forbidden due to the greater contribution to the Euclidean action (see Fig. 10).

The validity condition for weakly interacting instanton–anti-instanton pairs, in the adiabatic approximation, was discussed in Ref. 27.

The numerical analysis of the transcendental equation (35) reveals interesting features for a transition region between the tunneling regimes, i.e., a fine structure near the first bifurcation point for the antiparallel transfer. The numerical results are presented in Fig. 11. We found that, in addition to the first bifurcation point characterized by the two solutions [Fig. 11(a)], there exist additional bifurcation points at lower temperatures, i.e., the 4 pairs [Fig. 11(b)], the

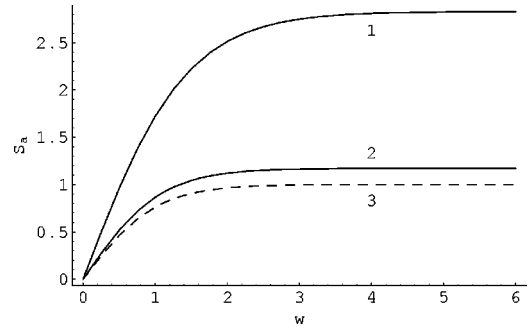


FIG. 10. Instanton action for antiparallel tunneling ($\varepsilon=0$, $a=b$) as a function of an inverse temperature at the two different values of the interaction parameter: $S_a = S/(4\omega a^2)$, $w = \omega\beta/4$. (1) $\tilde{\alpha}^* = 0.5$, (2) $\tilde{\alpha}^* = 0.1$, and (3) a dashed line corresponds to the action (33) for the parallel transition ($\varepsilon=0$, $a=b$).

6 pairs [Fig. 11(c)], and there are even 12 pairs of additional solutions at $\beta^* = 19.2009$ ($\alpha^* = 0.05$), etc. We refer to this phenomenon as a multiplication of bifurcations or a *cascade of bifurcations*. Such an effect resembles a scenario of transition to chaos.

Although the synchronous regime is preferred due to the minimal instanton action, in a certain temperature range its value is comparable with those of corresponding to the cascade solutions. As a result, *quantum fluctuations* of a non-regular character occur in contrast to parallel transfer. Antiparallel tunneling is, thus, characterized by the instability of the transition due to the synchronous to asynchronous behavior. Such instabilities are similar to a continuous second-order phase transition, while parallel tunneling is viewed as a step process similar to the phase transition of first order (see Fig. 6). The dependences shown in Figs. 7 and 8, $\beta_c(\alpha)$ and $\alpha_c(\beta)$, for antiparallel transfer are found to be of the same character as those of parallel transfer.

In summary, our investigation reveals a quite complicated fine structure of the transition for parallel and antiparallel tunneling of two particles with different degenerate trajectories leading to the bifurcation cascade.

VI. EFFECT OF A PROMOTING MODE

In this section, we study the effect of a heat bath on the tunneling transition of two interacting particles. In many tunneling reactions, the interaction with a vibrational subsystem can often be approximated by the interaction with a single vibrational mode (a so-called promoting mode). As follows from Eq. (12), a heat bath affects only the dynamics of the center of mass ($q_1 = q_2$). Therefore, in the case of antiparallel motion, the medium does not affect the rate constant, while for parallel tunneling it essentially contributes to the transfer rate. For both parallel and antiparallel transfer, the bilinear interaction of particles with a single oscillator can make a qualitative change in the character of tunneling.

At small values of the interaction parameter between the two tunneling particles dissipative effects become important.²⁷ In two dimensions the dissipative effects are more pronounced for parallel rather than antiparallel tunneling. The latter increases with temperature with a considerable contribution to the prefactor. In the present work, we are

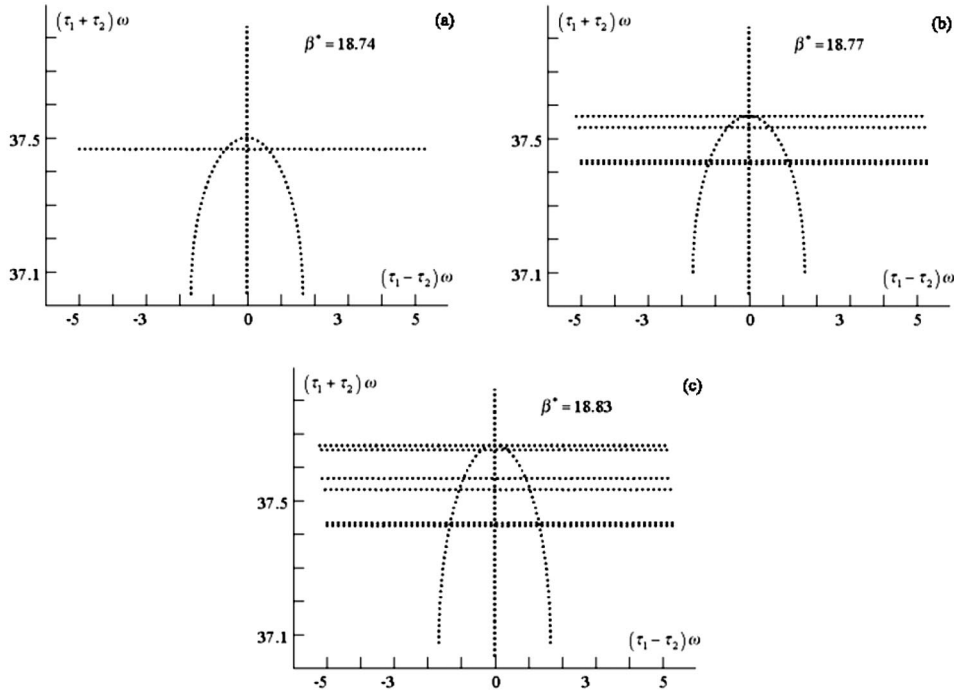


FIG. 11. Numerical solutions of the transcendental equation (35). In addition to the studied solution $\tau_1 = \tau_2$, with respect to β , there are the additional solutions, $\tau_1 \neq \tau_2$, shown in panels (a), (b), and (c), which correspond to one, four, and six (pairs) additional solutions, respectively.

interested in the tunneling rate assuming only exponential evolution of the transition probability. However, nonexponential evolution can occur in a nonequilibrium environment.^{35–38} Such a case is not discussed here. Accordingly, a reservoir is assumed to be in thermodynamic equilibrium; i.e., the tunneling transition is rather slow compared to the thermodynamic relaxation. Thus, we assume that dissipation affects the value of instanton action only.

For the case of antiparallel tunnel transfer, the action

(25) can be calculated with the following vibronic Green's function:

$$D(v_n) = -\frac{C^2}{v_n^2 + \omega_L^2}, \quad (41)$$

where ω_L is the frequency of the vibrational mode. After some tedious calculations, one obtains the following expression for the instanton action (25):

$$\begin{aligned} S = & \frac{2\omega^4(a^2 - b^2)\tau_0}{\Omega_0^2} - \frac{2\omega^4(a+b)^2}{\beta} \left\{ -\frac{\beta \sinh[\Omega_0(\beta/2 - \tau_0)] \sinh(\Omega_0\tau_0)}{2\Omega_0^3 \sinh(\Omega_0\beta/2)} + \sum_{i=1}^2 \frac{\beta(\Omega_i^2 - \omega_L^2) \cosh[\Omega_i(\beta/2 - \tau_0)] \cosh(\Omega_i\tau_0)}{(-1)^i 2\Omega_i^3 (\Omega_1^2 - \Omega_2^2) \sinh(\Omega_i\beta/2)} \right. \\ & + \frac{\beta\varepsilon}{4(\omega^2 - 2C^2/\omega_L^2)} - \frac{\beta\varepsilon}{4\Omega_0^2} + \frac{\beta \sinh(\varepsilon\Omega_0)}{4\Omega_0^3} + \sum_{i=1}^2 \frac{\beta(\Omega_i^2 - \omega_L^2) \sinh(\varepsilon\Omega_i)}{(-1)^i 4\Omega_i^3 (\Omega_1^2 - \Omega_2^2)} + \frac{\beta \cosh(\varepsilon\Omega_0)}{4\Omega_0^3 \sinh(\beta\Omega_0/2)} \{ \cosh[\Omega_0(\beta/2 - 2\tau_0)] \\ & \left. - \cosh(\Omega_0\beta/2) \} - \sum_{i=1}^2 \frac{\beta(\Omega_i^2 - \omega_L^2) \cosh(\varepsilon\Omega_i)}{(-1)^i 4\Omega_i^3 (\Omega_1^2 - \Omega_2^2) \sinh(\beta\Omega_i/2)} \{ \cosh[\Omega_i(\beta/2 - 2\tau_0)] + \cosh(\Omega_i\beta/2) \} \right\}. \quad (42) \end{aligned}$$

Here, we have introduced the following notation:

$$\Omega_0^2 = \omega^2 - \alpha^2, \quad \Omega_1^2 = \frac{1}{2}[\omega^2 + \omega_L^2 + \sqrt{(\omega^2 - \omega_L^2)^2 + 8C^2}],$$

$$\Omega_2^2 = \frac{1}{2}[\omega^2 + \omega_L^2 - \sqrt{(\omega^2 - \omega_L^2)^2 + 8C^2}].$$

For the parallel tunneling transition, a corresponding action can be found in a similar way. The action (27) as a function of the parameters $\varepsilon^* = \tau_1 - \tau_2$ and $\tau^* = (\tau_1 + \tau_2)/2$, with vibronic frequency ω_L and coupling constant C , yields (see also Ref. 27)

$$\begin{aligned}
S = & (a+b)(3a-b)\omega^2\tau^* - \frac{\omega^4(a+b)^2\varepsilon^*}{2(\omega^2-2\alpha)} - \frac{4\omega^2(a+b)^2\tau^{*2}}{\beta} - \frac{4\omega^4(a+b)^2\varepsilon^{*2}}{(\omega^2-2\alpha)\beta} \\
& - \frac{\omega^2(a+b)^2}{2\tilde{\gamma}} \sum_{i=1}^2 \frac{(-1)^i(\omega^2-x_{3-i})}{\sqrt{x_i}} \left(\coth\left(\frac{\beta\sqrt{x_i}}{2}\right) - \sinh^{-1}\left(\frac{\beta\sqrt{x_i}}{2}\right) \left\{ \cosh\left[\left(\frac{\beta}{2}-2\tau^*\right)\sqrt{x_i}\right] - \cosh\left[\left(\frac{\beta}{2}-\varepsilon^*\right)\sqrt{x_i}\right] \right. \right. \\
& + \left. \left. \frac{1}{2} \cosh\left[\left(\frac{\beta}{2}-2\tau^*-\varepsilon^*\right)\sqrt{x_i}\right] + \frac{1}{2} \cosh\left[\left(\frac{\beta}{2}-2\tau^*+\varepsilon^*\right)\sqrt{x_i}\right] \right\} \right) + \frac{\omega^4(a+b)^2}{2(\omega^2-2\alpha)^{3/2}} \left(-\coth\left(\frac{\beta}{2}\sqrt{\omega^2-2\alpha}\right) \right. \\
& + \left. \sinh^{-1}\left(\frac{\beta}{2}\sqrt{\omega^2-2\alpha}\right) \left\{ -\cosh\left[\left(\frac{\beta}{2}-2\tau^*\right)\sqrt{\omega^2-2\alpha}\right] + \cosh\left[\left(\frac{\beta}{2}-\varepsilon^*\right)\sqrt{\omega^2-2\alpha}\right] + \frac{1}{2} \cosh\left[\left(\frac{\beta}{2}-2\tau^*-\varepsilon^*\right)\sqrt{\omega^2-2\alpha}\right] \right. \right. \\
& \left. \left. + \frac{1}{2} \cosh\left[\left(\frac{\beta}{2}-2\tau^*+\varepsilon^*\right)\sqrt{\omega^2-2\alpha}\right] \right\} \right). \tag{43}
\end{aligned}$$

Here we have denoted

$$\begin{aligned}
x_{1,2} &= \frac{1}{2} \left(\omega^2 + \omega_L^2 + \frac{C^2}{\omega_L^2} \right) \mp \frac{1}{2} \tilde{\gamma}, \\
\tilde{\gamma} &= \sqrt{\left(\omega^2 + \omega_L^2 + \frac{C^2}{\omega_L^2} \right)^2 - 4\omega^2\omega_L^2}.
\end{aligned}$$

For particular values of the interaction constant α and in the absence of an interaction with the oscillator bath, the critical temperature T_c (at which the synchronous and asynchronous tunnel regimes interchange) is found from Eqs. (31) and (38). These equations can be generalized to a nonzero interaction with the promoting mode. Typically, the critical temperature is found to be in the range from 10 to 400 K. In glasses, T_c can be very small while for chemical reactions it can be rather large. Additionally, T_c depends on the mean distance between the particles and, therefore, on their concentration.

Quantum tunneling is important²⁸ when $k_B T_c / (\hbar\omega) \leq 1$. Therefore, the symmetry breaking effects can take place at relatively high temperatures depending on the ‘‘frequency’’ of a barrier. For example, for porphyrins the critical temperature T_c is estimated to be about 200 K.

VII. CONCLUSIONS

In the single-instanton approximation, we have calculated the Euclidean action (12) for the models characterized by the different adiabatic potential energy surfaces, (3), (4), and (5), and made a detailed comparative analysis of the tunneling rate for two interacting particles moving in parallel or antiparallel within a dissipative environment. We have

also assumed exponential evolution of the transition probability.^{27,35–38}

We have shown that the change in a tunneling regime from synchronous to asynchronous transfer for a parallel transition occurs as a step process, similar to a phase transition of first order, while for antiparallel transfer it resembles a second-order phase transition.

We have explained the effect of a *cleavage* in the experimentally observed^{24–26,33} temperature dependence of the reaction rate for two tunneling particles. It has been shown that the effect of symmetry breaking is stable for parallel and unstable for antiparallel transfer, as is observed experimentally for some porphyrin systems.^{24–26,33} We have found a complicated fine structure in the bifurcation region due to *quantum fluctuations* for parallel two-dimensional tunneling. For antiparallel tunneling, the contribution of 4, 6, 12, etc., pairs of trajectory becomes important, resembling the transition to *chaos*.

Additionally, we have studied the interaction of two particles with phonons. Such coupling essentially modifies the antiparallel and parallel transitions in different ways. As follows from Eq. (12), the interaction with the reservoir does not change the dynamics of the center of mass for the antiparallel motion, while it makes a significant contribution to the transfer rate for the parallel transfer. Finally, Eq. (31) determines the validity condition for temperatures beyond which stable two-dimensional synchronous tunneling correlations of all kinds occur.

ACKNOWLEDGMENTS

The authors would like to thank A. I. Larkin and B. I. Ivlev for the stimulating interest in this work.

*Also at Kazakhstan Division, Moscow State University, Moscow 119899, Russia. Electronic address: aringazin@mail.kz

†Electronic address: yurid@uwyo.edu

‡Electronic address: physics@diamond.stup.ac.ru

§Also at Institute for Basic Research, P.O. Box 1577, Palm Harbor,

FL 34682, USA. Electronic address: physics@diamond.stup.ac.ru

¹R. Meyer and R.R. Ernst, J. Chem. Phys. **86**, 784 (1987).

²A.O. Caldeira and A.J. Leggett, Phys. Rev. Lett. **46**, 211 (1981).

³I. Affleck, Phys. Rev. Lett. **46**, 388 (1981).

⁴P.G. Wolynes, Phys. Rev. Lett. **47**, 968 (1981).

- ⁵A.I. Larkin and Yu.N. Ovchinnikov, *Pis'ma Zh. Eksp. Teor. Fiz.* **37**, 322 (1983).
- ⁶B.I. Ivlev and Yu.N. Ovchinnikov, *Zh. Eksp. Teor. Fiz.* **93**, 668 (1987).
- ⁷H. Grabert and U. Weiss, *Z. Phys. B: Condens. Matter* **56**, 171 (1984).
- ⁸A.O. Caldeira and A.J. Leggett, *Ann. Phys. (N.Y.)* **149**, 374 (1983); A.J. Leggett, S. Chakravarty, A.J. Dorsey, M.P.A. Fisher, A. Garg, and W. Zwegler, *Rev. Mod. Phys.* **59**, 1 (1987).
- ⁹V.I. Mel'nikov, *Zh. Eksp. Teor. Fiz.* **87**, 663 (1984).
- ¹⁰H. Dekker, *Phys. Rep.* **80**, 1 (1981).
- ¹¹A. Schmid, *Ann. Phys. (N.Y.)* **170**, 333 (1986).
- ¹²A.D. Zaikin and S.V. Panyukov, *Zh. Eksp. Teor. Fiz.* **89**, 1890 (1985).
- ¹³Yu. Kagan and N.V. Prokof'ev, *Pis'ma Zh. Eksp. Teor. Fiz.* **43**, 434 (1986).
- ¹⁴H. Grabert and U. Weiss, *Phys. Rev. Lett.* **54**, 1605 (1985).
- ¹⁵M.Yu. Sumetskii, *Zh. Eksp. Teor. Fiz.* **89**, 618 (1985).
- ¹⁶Yu.N. Ovchinnikov, *Zh. Eksp. Teor. Fiz.* **94**, 365 (1988).
- ¹⁷B.I. Ivlev, *Zh. Eksp. Teor. Fiz.* **94**, 333 (1988).
- ¹⁸U. Weiss, *Quantum Dissipative Systems* (World Scientific, Singapore, 1993).
- ¹⁹H. Grabert, P. Schramm, and G.-L. Ingold, *Phys. Rep.* **168**, 115 (1988).
- ²⁰L. Gammaitoni, P. Hänggi, and P. Jung, *Rev. Mod. Phys.* **70**, 223 (1998).
- ²¹K. Yamamoto, *Prog. Theor. Phys.* **96**, 1147 (1996).
- ²²V.A. Benderskii and D.E. Makarov, *Phys. Rep.* **233**, 197 (1993).
- ²³J. Ankerhold and H. Grabert, *Phys. Rev. E* **61**, 3450 (2000); *Europhys. Lett.* **47**, 285 (1999).
- ²⁴Z. Smedarchina, W. Siebrand, and T.A. Wildman, *Chem. Phys. Lett.* **143**, 395 (1988).
- ²⁵Z. Smedarchina, W. Siebrand, and F. Zerbetto, *Chem. Phys.* **136**, 285 (1989).
- ²⁶K. Tokumura, Y. Watanabe, and M. Itoh, *J. Phys. Chem.* **90**, 2362 (1986).
- ²⁷Yu.I. Dakhnovskii, A.A. Ovchinnikov, and M.B. Semenov, *Zh. Eksp. Teor. Fiz.* **92**, 955 (1987).
- ²⁸Yu.I. Dakhnovskii and M.B. Semenov, *J. Chem. Phys.* **91**, 7606 (1989).
- ²⁹Yu.I. Dakhnovskii, A.A. Ovchinnikov, and M.B. Semenov, *Hadronic J.* **25**, 303 (2002).
- ³⁰V.A. Benderskii, E.V. Vetoshkin, and E.I. Kats, *Zh. Eksp. Teor. Fiz.* **122**, 746 (2002); cond-mat/0303275 (unpublished); V.A. Benderskii, E.V. Vetoshkin, E.I. Kats, and H.P. Trommsdorff, *Phys. Rev. E* **67**, 026102 (2003).
- ³¹H. Frauenfelder, in *Physics of Biological Systems: From molecules to species*, edited by H. Flyvbjerg, J. Hertz, M. H. Jensen, O. G. Mouritsen, and K. Sneppen (Springer, Berlin, 1997), p. 29.
- ³²K. Tagami, M. Tsukada, T. Matsumoto, and T. Kawai, *Phys. Rev. B* **67**, 245324 (2003).
- ³³V. M. Mamaev and V. V. Gorchakov, *Foundations of Chemical Dynamics: The Potential Energy Surfaces and Tunnel Dynamics* (DGU, Vladivostok, 1988).
- ³⁴D.J.W. Geldart and D. Neilson, *Phys. Rev. B* **67**, 205309 (2003).
- ³⁵M. Hornbach and Yu. Dakhnovskii, *J. Chem. Phys.* **111**, 5073 (1999).
- ³⁶Yu. Dakhnovskii, *J. Chem. Phys.* **111**, 5418 (1999).
- ³⁷D.G. Evans, A. Nitzan, and M.A. Ratner, *J. Chem. Phys.* **108**, 6387 (1998).
- ³⁸Yu. Dakhnovskii, V. Lubchenko, and P. Wolynes, *J. Chem. Phys.* **104**, 1875 (1996).